Electronic Supplementary Information

for

A possible way how to improve *in vitro* cytotoxicity of half-sandwich Os(II) complexes against A2780 cells

Pavel Štarha,[a] Zdeněk Trávníček,*[a] Radovan Herchel,[a] Pawel Jewula[a] and Zdeněk Dvořák[b]

[a] Department of Inorganic Chemistry, Regional Centre of Advanced Technologies and Materials, Faculty of Science, Palacký University Olomouc, 17. listopadu 12, 771 46 Olomouc, Czech Republic

[b] Department of Cell Biology and Genetics, Regional Centre of Advanced Technologies and Materials, Faculty of Science, Palacký University Olomouc, Šlechtitelů 27, 783 71 Olomouc, Czech Republic

Corresponding Author (Z.T.):

* E-mail: zdenek.travnicek@upol.cz.

Table of contents

Figures S1–S13.... 2

Tables S1–S6.....15

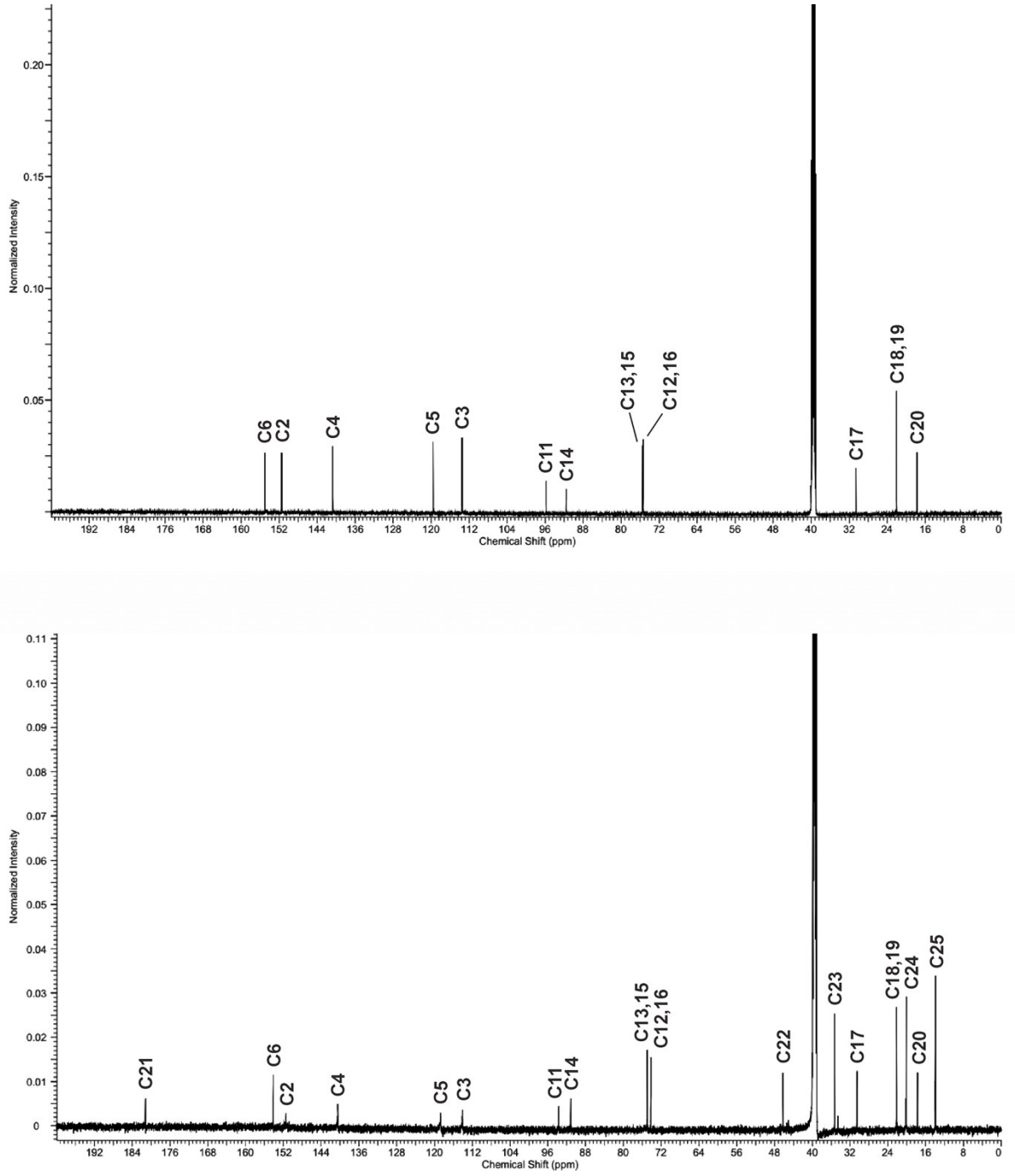

Figure S1. ^{13}C NMR spectra for the complexes **1-VP** (*bottom*) and **1-Cl** (*top*).

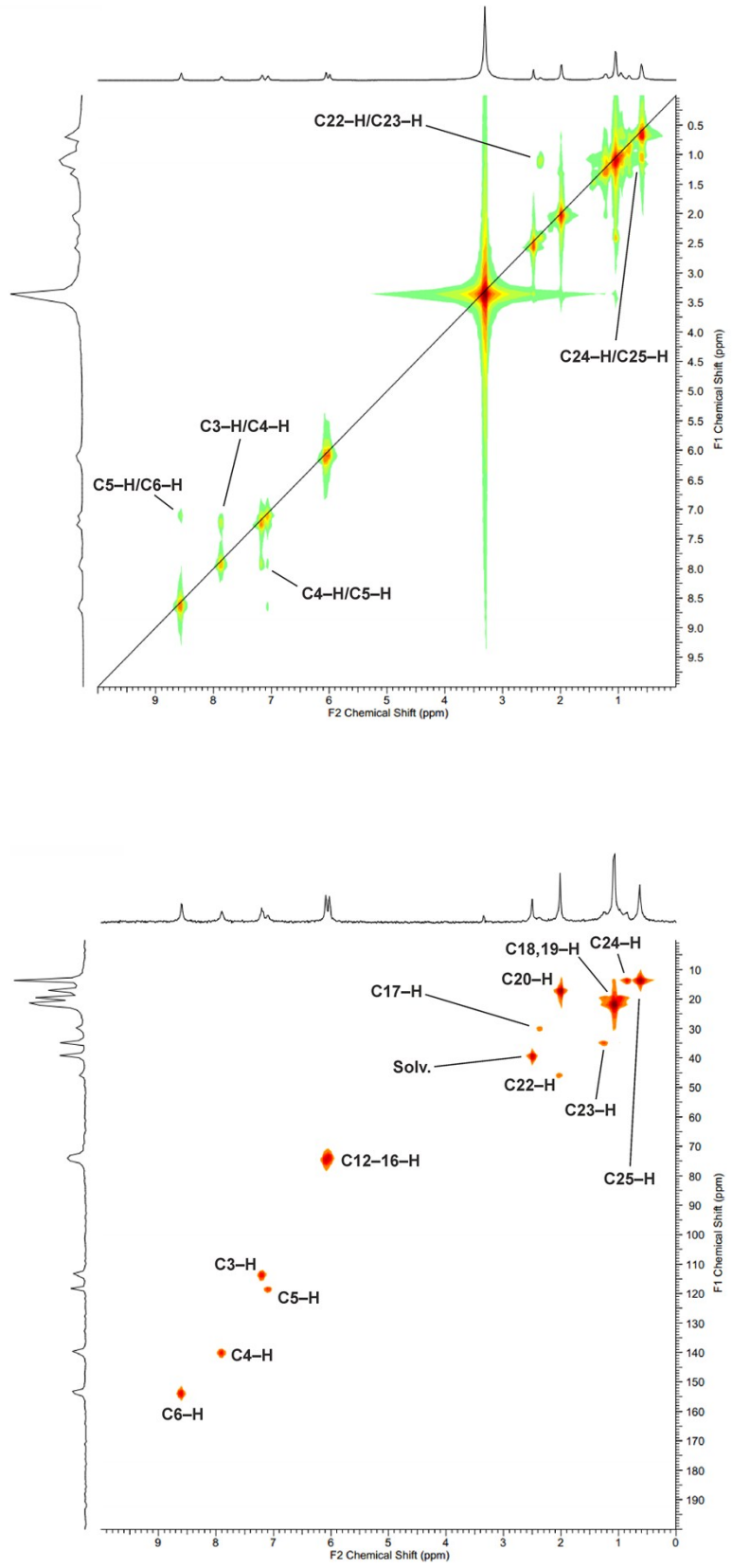

Figure S2. $^{1}H–^{1}H$ gs-COSY (*top*) and $^{1}H–^{13}C$ gs-HMQC (*bottom*) spectra of the complex **1-VP**.

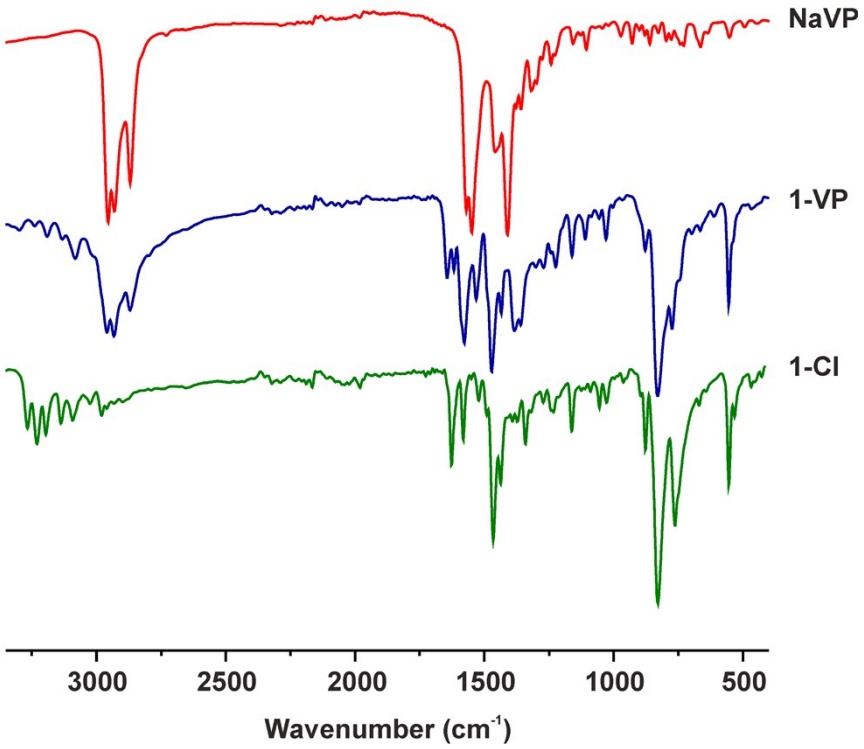

Figure S3. FTIR spectra of the complexes **1-Cl** (green) and **1-VP** (blue), given with sodium valproate (NaVP; red) for comparative purposes. IR (ν_{ATR}/cm^{-1}): 469, 532, 555, 670, 762, 830, 877, 896, 1026, 1055, 1162, 1237, 1273, 1341, 1372, 1393, 1437, 1466, 1492, 1522, 1582, 1627, 2980, 3025, 3092, 3137, 3196, 3230, 3266 for **1-Cl**, and 469, 555, 612, 665, 698, 774, 831, 879, 1003, 1029, 1056, 1110, 1161, 1224, 1244, 1270, 1302, 1360, 1385, 1435, 1473, 1533, 1578, 1618, 1643, 2870, 2933, 2959, 3082, 3191, 3240, 3298 for **1-VP**.

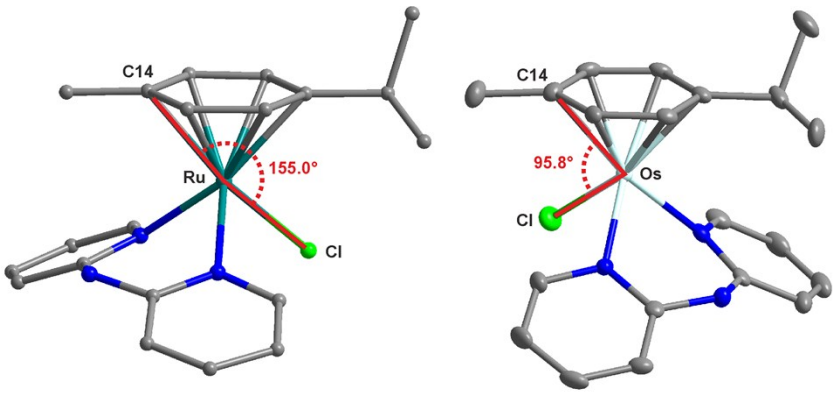

Figure S4. A comparison of the molecular structures of the complexes [Ru(η^6-*p*cym)(dpa)Cl]PF_6 (CSD refcode: IKEKUF; *left*)[1] and [Os(η^6-*p*cym)(dpa)Cl]BPh_4·CH_3OH (**1-Cl`**·CH_3OH; *right*), given with the <Cl–M–C14 bond angle (red lines) formed by the chlorido ligand, central atom (M = Ru or Os) and the C14 carbon atom of the *p*-cymene ring. The counterions (PF_6^-, BPh_4^-), CH_3OH molecule of crystallization and hydrogen atoms have been omitted for clarity. The value of the Cl–M–C14 bond angle equals 95.78(8)° and 155.01(7)° for the complex **1-Cl`**·$CH_3OH$, and [Ru(η$^6$-*p*cym)(dpa)Cl]$PF_6$, respectively, while the value of the Cl–M–C14–C20 torsion angle equals 33.5(3)°, and 101.2(2)° for the complex **1-Cl`**·CH_3OH, and [Ru(η^6-*p*cym)(dpa)Cl]PF_6, respectively.

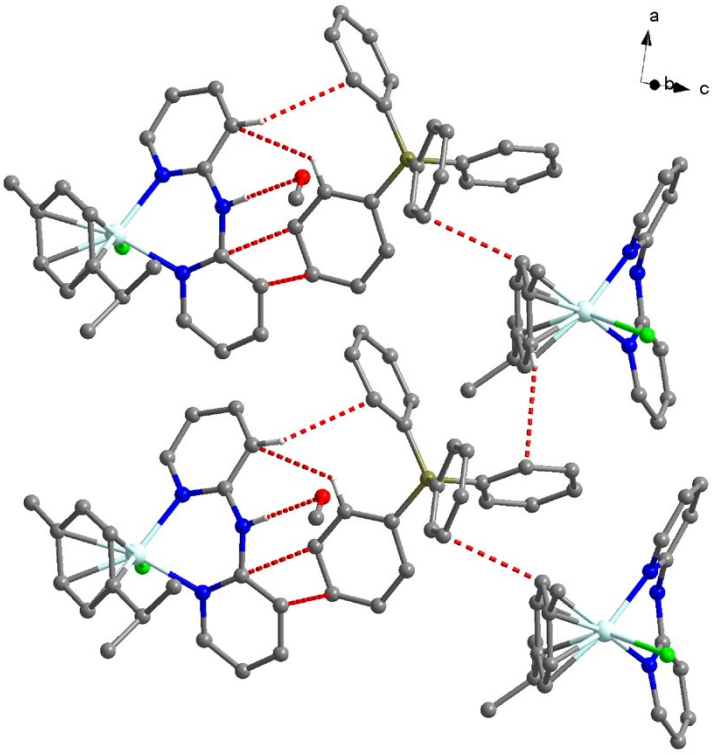

Figure S5. Part of the crystal structure of the complex **1-Cl`**·$CH_3OH$ with the N–H···O, C–H···C and C···C non-covalent contacts depicted by red dashed lines. The hydrogen atoms not involved in the depicted non-covalent contacts have been omitted for clarity. The dihedral angle between both pyridine rings of dpa of the complex **1-Cl`**·CH_3OH equals 39.24(11)°.

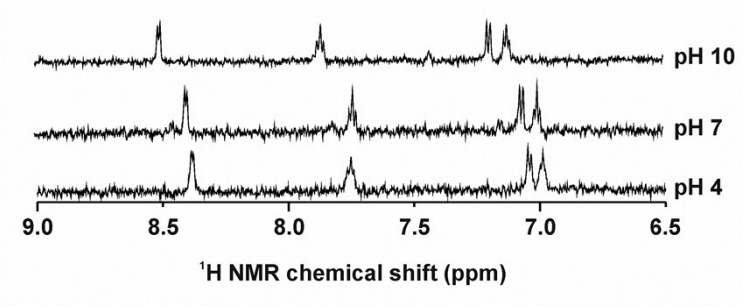

Figure S6. The representative parts of the ^{1}H NMR spectra (10% MeOD-d_4/90% D_2O) of the $[Os(\eta^6\text{-}p\text{cym})(dpa)(OD_2)]^{2+}$ (**1-OD$_2$**;pH 4 and 7) and $[Os(\eta^6\text{-}p\text{cym})(dpa)(OD)]^{+}$ (pH 10) species.

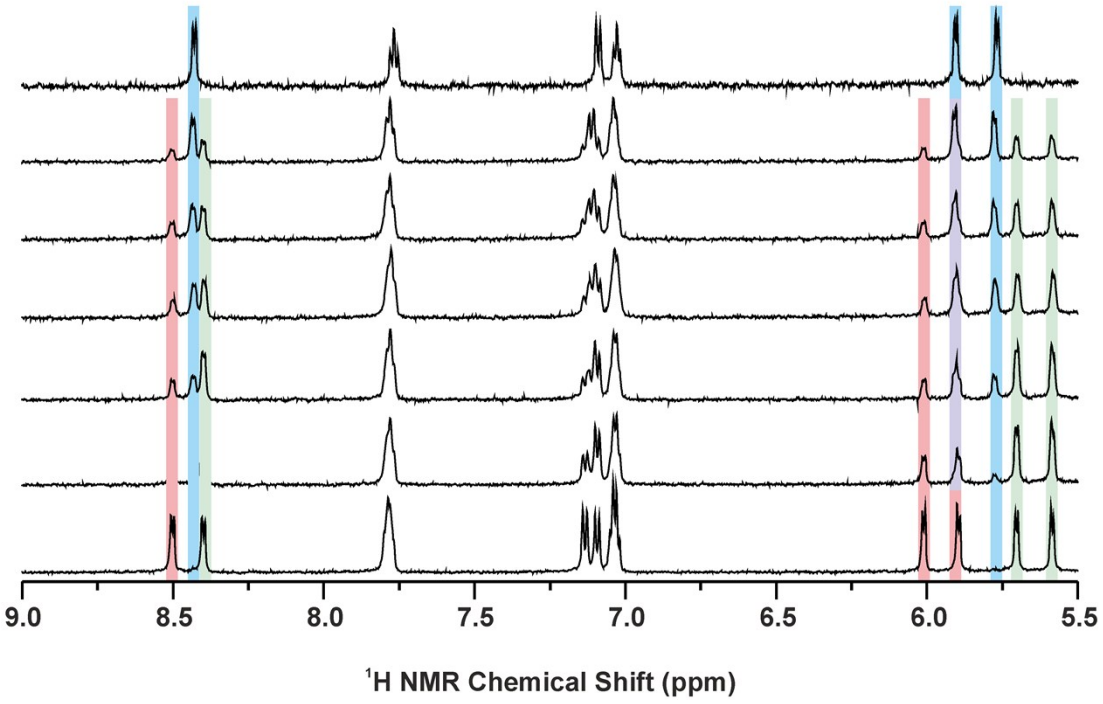

Figure S7. A comparison of the ^{1}H NMR spectra (5.5–9.0 ppm region) of **1-Cl** and **1-VP** in phosphate buffer, as observed at different time points. The signals of **1-Cl** are given in blue, **1-VP** is pink coloured and **1-OD$_2$** is given in green blue (violet coloured signals represent an overlay of the signals of **1-Cl** and **1-VP**).

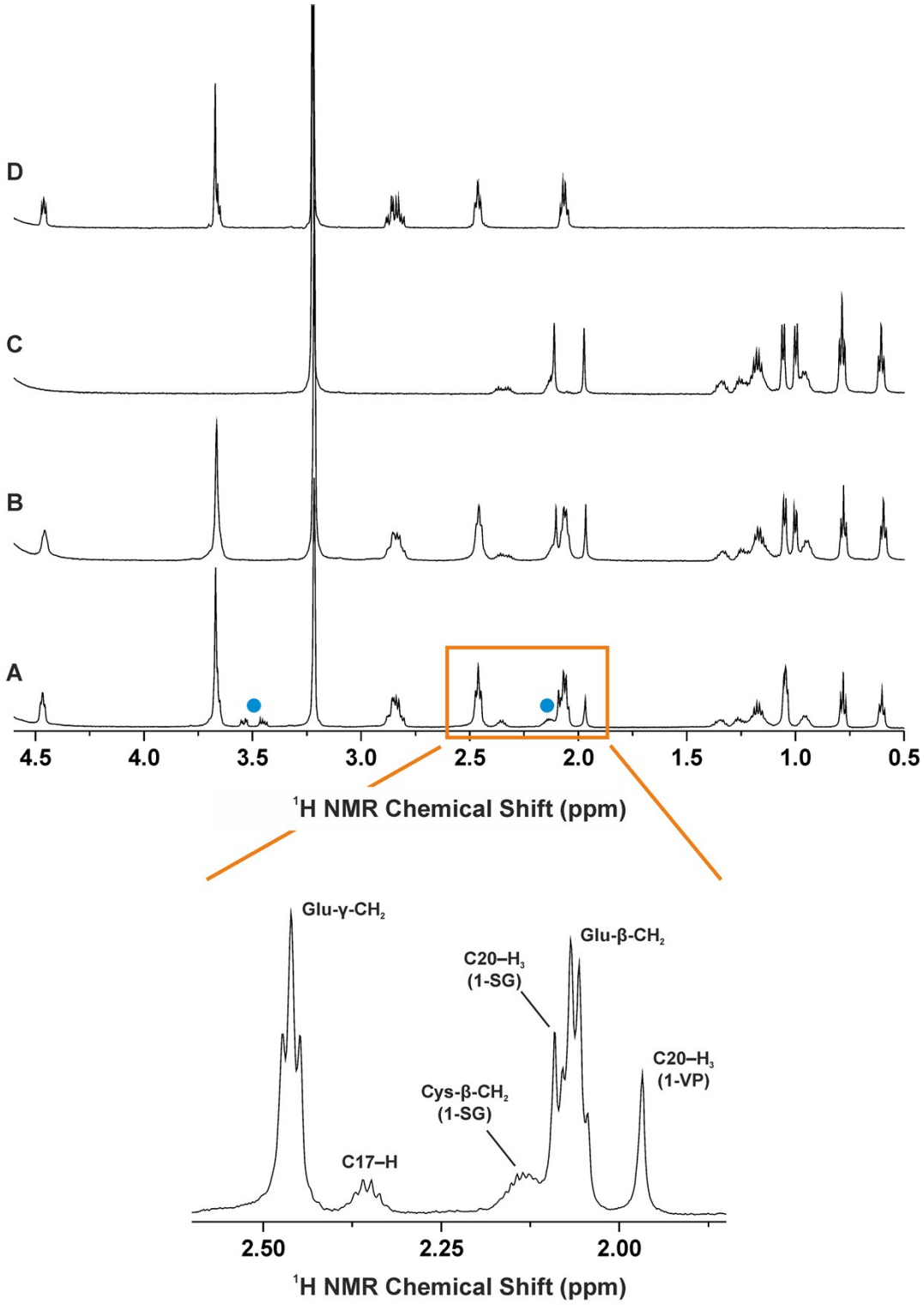

Figure S8. ^{1}H NMR spectra of the mixtures of **1-VP** with 2 mol equiv. of GSH (A, B) recorded either in the mixture of 0.1% KOD in 10% MeOD-d_4/90% D_2O (pH = 7.2; A and detail) or in phosphate buffer (B). The signals of Cys-α-CH and Cys-β-CH_2 are highlighted by blue colour. The spectra of the complex **1-Cl** in 10% MeOD-d_4/90% D_2O (C) and free GSH in phosphate buffer (D) are given for comparative purposes.

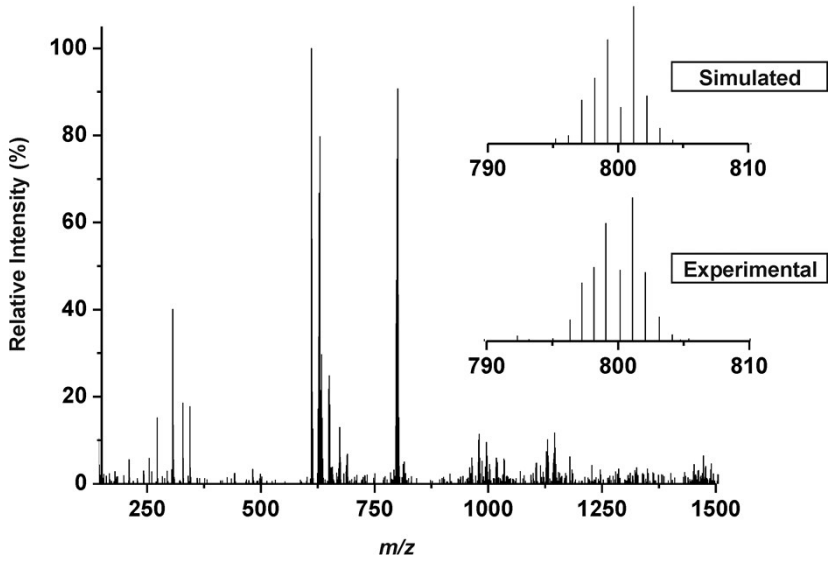

Figure S9. ESI– mass spectrum recorded on the mixture of the complex **1-VP** with 2 molar equiv. of GSH in 10% MeOH/90% H_2O with an addition of 0.1% KOH (pH = 7.2), with details of the peaks of the $\{[Os(p\text{cym})(dpa)(SG)]-2H\}^-$ species (**1-SG**; *inset bottom* - experimental data, *inset top* - simulated isotopic distribution].

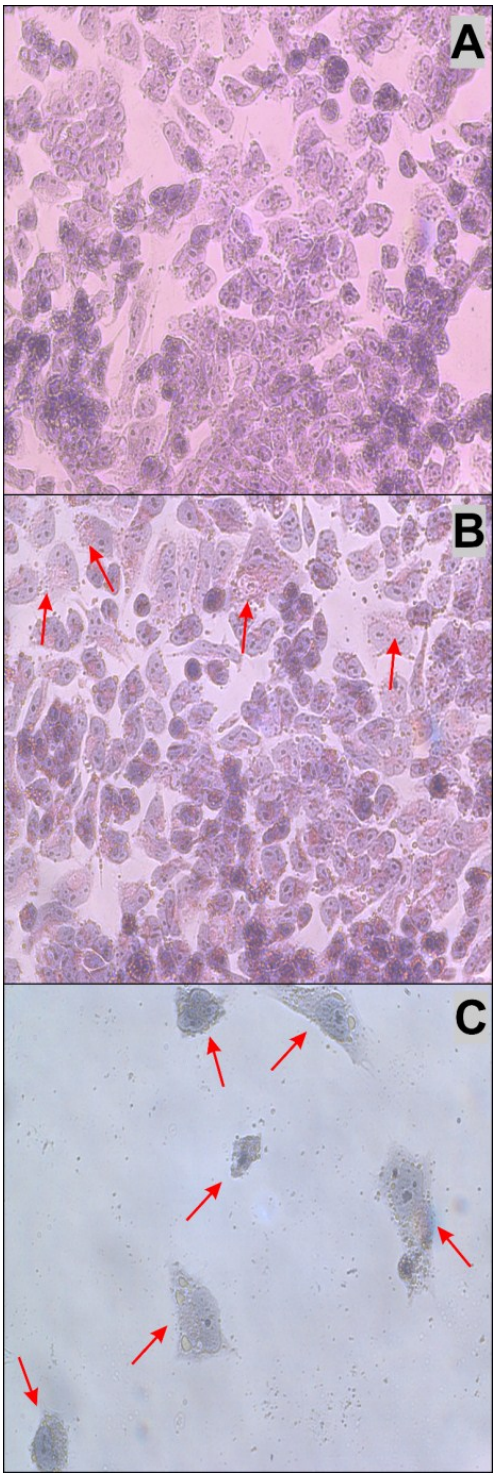

Figure S10. Representative photomicrographs (40×, original magnification) showing the morphological changes of the A2780 cells treated by the IC_{50} concentrations of the complex **1-VP** (**B**) and *cisplatin* (**C**; for comparative purposes) for 24 h with 72 h recovery time, given together with negative control (**A**; untreated cells).

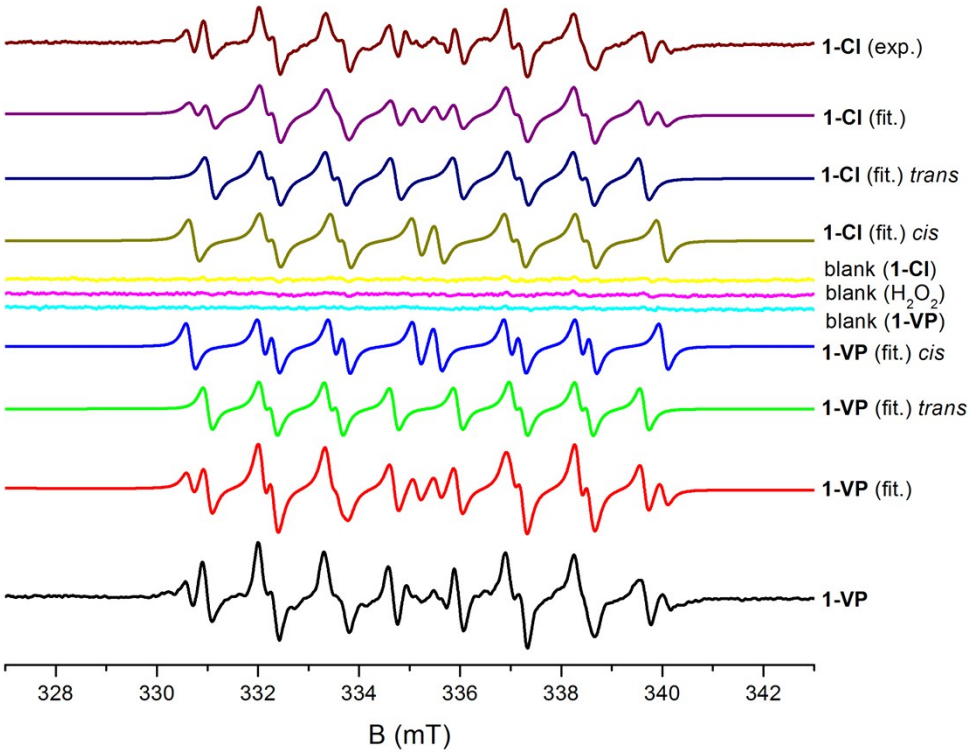

Figure S11. The results of EPR spin trapping experiments for **1-Cl** and **1-VP** given together with the fitted data and the experimental data of blank samples. The fitted parameters for **1-Cl**: g_{iso} = 2.006, A_{iso}(N) = 39.2 MHz, A_{iso}(P) = 136 MHz, A_{iso}(H) = 45.5 MHz for the *cis*-DEPMPO/OH and g_{iso} = 2.006, A_{iso}(N) = 36.5 MHz, A_{iso}(P) = 138 MHz, A_{iso}(H) = 30.0 MHz with the isomers ratio of 0.66 : 1. The fitted parameters for **1-VP**: g_{iso} = 2.006, A_{iso}(N) = 39.4 MHz, A_{iso}(P) = 137 MHz, A_{iso}(H) = 46.9 MHz for the *cis*-DEPMPO/OH and g_{iso} = 2.007, A_{iso}(N) = 36.4 MHz, A_{iso}(P) = 139 MHz, A_{iso}(H) = 30.7 MHz with the isomers ratio of 0.53 : 1.

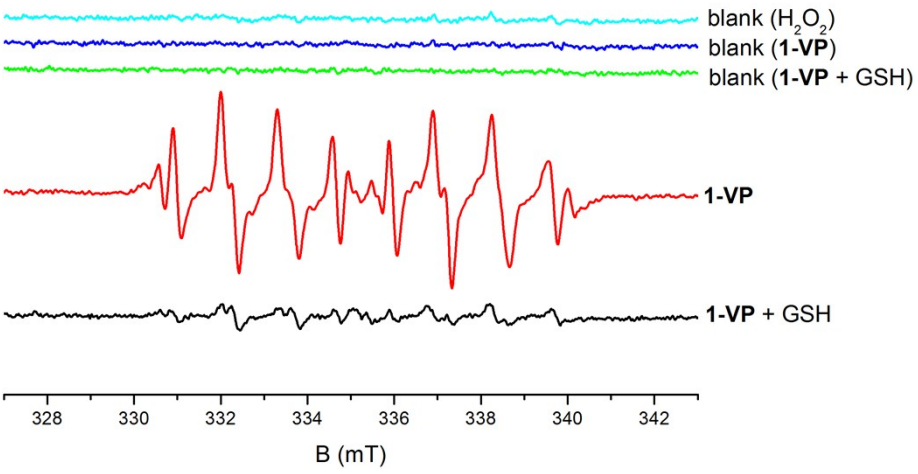

Figure S12. The results of EPR spin trapping experiments for the system containing **1-VP** (*red*) and its mixture with 2 mol equiv. of the reduced glutathione (GSH; *black*) measured in the mixture of DMF and 75 mM PBS in water (1:3, *v/v*).

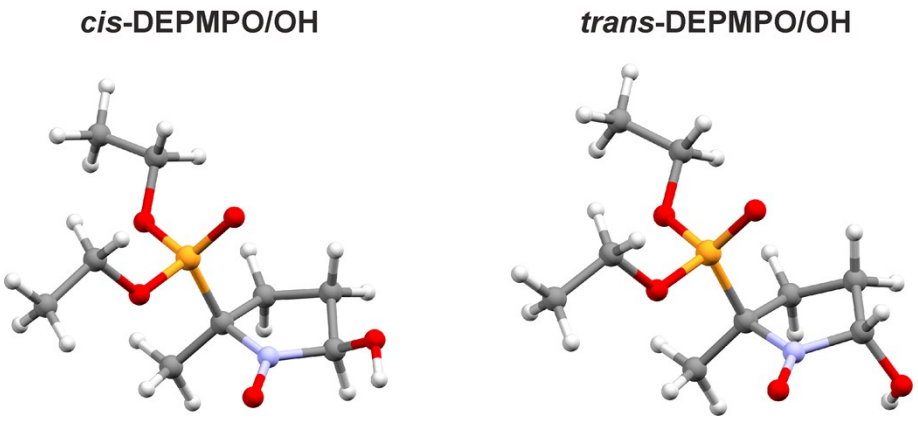

Figure S13. The DFT optimized molecular structures of *cis*- and *trans*-diastereoisomers of DEPMPO/OH radical with the DFT calculated parameters of *g*-value and the isotropic hyperfine splitting parameters, as follows: g_{iso} = 2.006, A_{iso}(N) = 28.7 MHz, A_{iso}(P) = 148 MHz and A_{iso}(H) = 55.7 MHz for *cis*-DEPMPO/OH, and g_{iso} = 2.006, A_{iso}(N) = 26.5 MHz, A_{iso}(P) = 158 MHz and A_{iso}(H) = 32.9 MHz for *trans*-DEPMPO/OH.

Table S1. Crystal data and structure refinements for the complex **1-Cl`**·CH_3OH.

Empirical formula	$C_{45}H_{47}BClN_3OOs$
Formula weight	882.31
Temperature (K)	120(2)
Wavelength (Å)	0.71073
Crystal system,	Monoclinic, *Cc*
a; *b*; *c* (Å)	16.9295(7); 9.6722(4); 23.1376(8)
α; *β*; *γ* (°)	90.0; 91.1460(10); 90.0
V (Å^3)	3787.9(3)
Z, D_{calc} (g cm^{-3})	4, 1.547
Absorption coefficient (mm^{-1})	3.477
Crystal size (mm)	0.200 × 0.160 × 0.140
F (000)	1776
θ range for data collection (°)	2.407 to 27.477
Index ranges (*h; k; l*)	-21 ≤ *h* ≤ 21; -12 ≤ *k* ≤ 12; -29 ≤ *l* ≤ 30
Reflections collected	44488
Independent reflections	8268 [*R*(int) = 0.0295]
Data/restraints/parameters	8268/2/477
Goodness–of–fit on F^2	0.921
Final *R* indices [*I*>2σ(*I*)]	R_1 = 0.0144, wR_2 = 0.0296
R indices (all data)	R_1 = 0.0157, wR_2 = 0.0299
Largest peak and hole (e Å^{-3})	0.542 and -0.685

Table S2. Selected lengths (Å) and angles (°) of non-covalent contacts detected in the crystal structure of **1-Cl`**·CH_3OH.

Contact	*d*(D–H) (Å)	*d*(H···A) (Å)	*d*(D–H···A) (Å)	<(D–H···A) (°)
N2–H2A···O	0.84(4)	2.03(4)	2.865(4)	179(4)
N2–H2A···O	0.84(4)	2.85(4)	3.605(5)	151(3)
C3A–H3A···C31^{i}	0.95	2.78	3.557(4)	140.0(2)
C13–H13A···C65^{ii}	0.95	2.89	3.667(4)	140.1(2)
C43–H43A···C51^{iii}	0.95	2.75	3.664(5)	161.2(2)
C43–H43A···C52^{iii}	0.95	2.86	3.575(4)	132.5(2)
C51–H51A···C3A^{iii}	0.95	2.76	3.430(5)	128.7(3)
C61–H61A···C20^{iv}	0.95	2.79	3.579(4)	141.0(2)
O–HW···Cg^{i}	0.84	2.68	3.460(2)	155.61(14)
C2···C52^{i}			3.34	
C3···C53^{i}			3.38	
C15···C41			3.39	

Symmetry codes: i) x, 1-y, z+0.5; ii) x-0.5, y+0.5, z; iii) x, 1+y, z; iv) x, y-1, z.

Table S3. Cell populations (%) in the cell cycle phases (PI/RNase staining of the A2780 cells treated for 2 or 24 h by the IC_{50} concentrations of the complexes **1-VP** and **1-Cl**, negative control (untreated cells) and *cisplatin* involved in the studies for comparative purposes. The data are given as arithmetic mean from three independent experiments.

	sub-G_1	G_0/G_1	S	G_2/M
2 h exposure				
1-Cl	0.8±0.1	68.4±0.5	10.9±0.6	18.4±0.1
1-VP	0.7±0.1	67.5±0.3	10.3±0.8	20.7±1.4
Cisplatin	0.7±0.1	65.8±2.9	12.1±0.7	20.5±2.3
Negative control	0.6±0.1	65.7±0.6	12.4±0.1	19.8±0.5
24 h exposure				
1-Cl	1.3±0.1	57.4±1.0	11.4±2.1	29.8±1.6
1-VP	1.1±0.1	62.4±0.7	9.6±0.3	26.6±0.3
Cisplatin	4.6±0.3	42.0±0.5	12.9±1.5	40.5±1.8
Negative control	1.2±0.1	60.2±0.8	10.4±0.8	28.0±0.3

Table S4. The results (given as % populations) of flow cytometry studies of the induction of apoptosis, studied at the A2780 cells using the treatment by the IC_{50} concentrations of **1-Cl** (59.9 μM) and **1-VP** (20.9 μM) for 2 and 24 h. The untreated A2780 cells were employed as the negative control and the cells treated with *cisplatin* (IC_{50} concentration) and *staurosporine* (1 μg/mL concentration) were studied for comparative purposes. The data are given as arithmetic mean±SD from three independent experiments. LL, lower left; LR, lower right; UL, upper left; UR, upper right.

	LL quadrant (FL1−/FL2−)	LR quadrant (FL1+/FL2−)	UR quadrant (FL1+/FL2+)	UL quadrant (FL1−/FL2+)
2 h exposure				
1-Cl	55.8±0.9	22.9±0.4	18.4±0.4	2.9±0.7
1-VP	67.2±0.2	20.2±0.1	10.7±0.2	1.9±0.1
Cisplatin	62.2±0.2	20.2±0.6	15.2±0.3	2.5±0.6
Staurosporine	86.0±1.3	1.2±0.4	1.0±0.3	11.9±0.8
Negative control	93.5±1.2	1.5±0.2	0.5±0.1	4.9±0.9
24 h exposure				
1-Cl	18.3±2.4	55.6±3.5	22.9±5.6	3.2±0.8
1-VP	15.6±3.2	51.6±0.9	26.8±3.1	6.1±0.7
Cisplatin	35.4±1.3	28.5±3.2	27.6±0.1	8.5±2.2
Staurosporine	16.0±1.1	44.3±2.7	36.0±1.2	3.7±1.2
Negative control	93.3±0.9	1.5±0.3	0.5±0.1	4.8±0.6

Table S5. The results (given as % populations) of flow cytometry studies of the induction of total reactive oxygen species (ROS) and superoxide production, studied in the A2780 cells using the treatment by the IC_{50} concentrations of the complexes **1-Cl** and **1-VP** for 24 h. The untreated A2780 cells were employed as the negative control, while the pyocyanine-treated cells represent the positive control. The data are given as arithmetic mean±SD from three independent experiments. LL, lower left; LR, lower right; UL, upper left; UR, upper right.

	LL quadrant (FL1−/FL2−)	LR quadrant (FL1+/FL2−)	UR quadrant (FL1+/FL2+)	UL quadrant (FL1−/FL2+)
1-Cl	<0.1	0.5±0.1	99.0±0.1	0.5±0.1
1-VP	<0.1	<0.1	99.9±0.1	<0.1
Positive control	<0.1	<0.1	99.9±0.1	<0.1
Negative control	99.8±0.1	<0.1	<0.1	<0.1

Table S6. The results (given as % cell populations) of flow cytometry studies of the mitochondrial membrane potential changes, studied at the A2780 cells using the treatment by the IC_{50} concentrations of the complexes **1-Cl** (59.9 μM) and **1-VP** (20.9 μM) (and *cisplatin* for comparative purposes) for 24 h. The untreated A2780 cells were employed as the negative control, while the CCCP-treated cells represent the positive control. The data are given as arithmetic mean±SD from three independent experiments.

	FL-2 Orange Fluorescence	
	Low	High
1-Cl	16.1±4.9	83.9±4.9
1-VP	23.7±6.2	76.1±6.2
Cisplatin	43.1±3.9	56.7±3.9
Positive control (CCCP)	98.6±0.1	1.3±0.1
Negative control	1.6±0.2	98.4±0.2

References:

[1] C. Romain, S. Gaillard, M. K. Elmkaddem, L. Toupet, C. Fischmeister, C. M. Thomas and J. L. Renaud, *Organometallics* 2010, **29**, 1992.